Pressure-controlled motion of single polymers through solid-state nanopores

Bo Lu[1]‡, David P. Hoogerheide[2]‡, Qing Zhao[1,]*, Hengbin Zhang[1], Zhipeng Tang[1], Dapeng Yu[1,]*, and Jene A. Golovchenko[2,]*

[1]State Key Laboratory for Mesoscopic Physics and Electron Microscopy Laboratory, School of Physics, Peking University, Beijing 100871, People's Republic of China

[2]Department of Physics, Harvard University, Cambridge, Massachusetts 02138, USA

ABSTRACT: Voltage-biased solid-state nanopores are well established in their ability to detect and characterize single polymers, such as DNA, in electrolytes. The addition of a pressure gradient across the nanopore yields a second molecular driving force that provides new freedom for studying molecules in nanopores. In this work, we show that opposing pressure and voltage bias enables nanopores to detect *and resolve* very short DNA molecules, as well as to detect near-neutral polymers.

KEYWORDS: Solid-state nanopores, pressure gradient, DNA single-molecule detection, near neutral molecule detection, short molecule discrimination

Charged single molecules of DNA can be detected and characterized with a voltage-biased solid-state nanopore immersed in an electrolyte solution.[1] This has stimulated intense research towards understanding and utilizing this nano-device for the analysis of a wide variety of charged polymer molecules.[2-7] Recent success using protein-based nanopores in lipid membranes for DNA sequencing,[8-11] after many years of effort, is an encouraging indicator of the potential scientific and commercial impact of nanopore devices.

Nanopore single-molecule detection is currently based on the dual role played by a voltage bias induced electric field near the nanopore. This field induces charged polyelectrolyte molecules to approach and pass through the nanopore, and it provides a measurable ionic current that is sensitive to the presence and nature of the molecule while in the pore. This method has limitations. First, very short, highly charged polymers like DNA pass through the pore so quickly that their lengths cannot be resolved or, in the worst case, their presence not even detected. Secondly, molecules of little or no charge are not even attracted to uncharged pores and hence will not be detected.

We show here that a pressure-induced fluid flow, in and near the nanopore, provides an additional force to control the motion of the molecule through the pore. This pressure-derived force, combined with the voltage bias, enables solid-state nanopores to detect and characterize very short molecules, near-neutral molecules, and molecules with varying charge polarities (e.g. proteins) along their length. For uniformly charged polymers like DNA, the pressure-derived force can be countered by the voltage-derived force to slow the molecule motion without reducing the ionic current signal. Below, we present model predictions that inspired the experiments we performed, and experimental data that show the role of applied pressure on DNA translocation in voltage-biased nanopores. We also demonstrate the ability to detect and resolve

short DNA molecules using pressure-voltage force balancing. Finally, we show the use of pressure to detect and characterize near-neutral single molecules with a nanopore. We finish with a discussion summarizing and expanding on the new capabilities arising from the use of pressure in nanopore devices.

Figure 1a shows the configuration of a conventional voltage-biased nanopore experiment augmented by an applied pressure differential across the nanopore and its membrane. The passage ("translocation") of individual DNA molecules through the nanopore is monitored by the change in the ionic current during its passage. Nanopores were fabricated in freestanding membranes of 80-nm thick low stress silicon nitride by focused electron beam drilling.[12] The nanopore was mounted in a fluidic cell, capable of withstanding several atmospheres of applied pressure. The membrane containing the nanopore separated two electrically isolated electrolyte-filled reservoirs in the cell. The electrolyte was 1.6 M KCl buffered at pH 9 by 10 mM tris buffer, unless specified otherwise. Divalent ions were complexed by 1 mM EDTA to prevent DNA conglomeration and surface adhesion. DNA was injected into one side of the sample cell, which was subsequently brought to the desired pressure by regulated compressed air or nitrogen. The other side of the cell was left open to the atmosphere. The pressure drop across the membrane is denoted as ΔP. External electronics providing voltage bias and current sensing were coupled to the electrolyte reservoirs with Ag/AgCl electrodes. All voltages are referenced to the grounded electrode on the high-pressure side of the cell. In this configuration, positive pressures and voltages both facilitate translocation of DNA introduced on the grounded side of the cell, while negative pressures and voltages retard translocation. More details of the experiments can be found in the Methods section.

Figure 1b presents the computer modeled forces on a DNA molecule, assumed parallel to the axis of the pore, vs. its radial distance from the pore center. The calculations refer to a pore of 10 nm diameter immersed in 1.6 M KCl at pH 9 and are performed using the Poisson-Boltzmann-Navier-Stokes approach described previously[13], augmented by appropriate pressure boundary conditions far from the pore. Included are predictions for voltage-derived forces (including the viscous effects of electroosmotic flow[14, 15]), pressure-derived viscous forces due to induced fluid flow, and a combination of the two. The voltage-derived forces increase near the pore walls because the electroosmotic flow around the molecule, which reduces the net force, is suppressed by the no-slip boundary conditions on the pore walls. Clearly modest applied pressures ($\Delta P \sim 1$ atm) should have a dramatic effect on DNA motion through the pore. The maximum of the parabolic pressure force is predicted to be proportional to the square of pore radius, as expected from Poiseuille flow. By contrast, voltage-derived forces do not depend strongly on pore size; for a 10 nm pore, a change in pore size of 25% results in only a slight decrease (11%) of the voltage-derived force.[13, 15]

Figure 2a shows an experimentally obtained density histogram of ionic current blockage vs. translocation event durations for 3.27 kbp double-stranded DNA (dsDNA) translocations with a bias of $V = +100$ mV and zero applied differential pressure, $\Delta P = 0$. Typical current trace data are shown in Figure S1a of the Supporting Information. These data reproduce typical distributions presented previously for molecules of similar length.[16] The nanopore diameter was ~10 nm and the conductance was 67 nS in the 1.6 M KCl electrolyte used for all the experiments in this work. The rms noise level was 10.9 pA at $V = 100$ mV. All noise levels are deduced from current noise power spectra integrated from 200 Hz and 40 kHz, as shown in Figure S2. Molecules were captured at an average rate of 50 per minute.

To demonstrate the role of pressure in molecule translocation, we then applied $\Delta P = 2.40$ atm and $V = -90$ mV across a pore of 43 nS conductance. Typical data are shown in Figure S1b. The rms noise level at $V = -90$ mV was 10.7 pA. The results are shown in Figure 2b. In this case the molecules pass through the pore only because the pressure-derived force exceeds the opposing voltage-derived force. The average speed of the DNA through the nanopore for these conditions is an order of magnitude lower than in the conventional voltage-driven result reported in Figure 2a, while the capture rate of 10 events per minute is about a factor of 5 lower. This factor of 2 for the ratio of the reduction in the capture rate to the reduction in average speed is typical for these experiments. The mean translocation time for unfolded events, selected as previously described,[17] increases from 115 to 950 μs, as shown in the distributions in Figure 2c. Further attempts to balance the pressure- and voltage-derived forces have resulted in additional slowing, up to a factor of about 20. When the net force is reduced by this amount, stochastic effects become significant. The result is a complex trapping behavior near the pore that will be presented elsewhere.

One notable difference between the density histograms shown in Figure 2a and Figure 2b is the behavior of "folded events," which have higher average current blockage than unfolded events.[5] In the voltage-only translocation experiment shown in Figure 2a, the molecules that are captured from a fold at their center go through the nanopore in approximately half the time of the unfolded molecules. This occurs because the force in the nanopore is positive over the entire cross-section of the pore (see Figure 1b), and the average force on the two strands is approximately double that of a single strand. The drag of two strands is also double that of one, but the length is half as long, so the translocation time is about half that of the unfolded molecules. Figure 2b, on the other hand, shows that in a nanopore biased with both pressure and

voltage, the translocation times of folded molecules are as long as or longer than those of unfolded molecules. This occurs because the direction of the net force reverses if the molecule departs significantly from the axis of the pore (see Figure 1b). When two DNA strands are in the pore, they repel each other such that one or both are always likely to be displaced from the pore axis. In the case where the pressure- and voltage-derived forces are well balanced, the net force on the two strands may thus be less than that on a single strand. This slows translocation of folded molecules, resulting in the observed increased translocation times for folded molecules.

One of the advantages of slowing molecule motion with pressure in the presence of a high opposing electric field is the ability to detect *and resolve* the lengths of much shorter molecules in a solid-state pore than has previously been possible. When translocating molecules using only a voltage bias, the difficulty of resolving short molecule lengths comes from the poor signal to noise connected with the high bandwidth needed to resolve short blockage signals. In Figure 3a, we show the density histogram for translocation of only 615 bp dsDNA molecules in a nanopore of conductance 60 nS, using $\Delta P = 2.44$ atm and $V = -100$ mV. The rms noise level was 11.9 pA at $V = -100$ mV.

In Figure 3b, we resolve a mixture of 615 bp and 1.14 kbp dsDNA molecules in a nanopore of conductance 43 nS, using $\Delta P = 2.56$ atm and $V = -100$ mV. The rms noise level was 15.8 pA. The peak separation of about 70 μs is significantly greater than the peak widths (about 40 μs), all determined from weighted least-squares fits of two Gaussians ($\chi^2 = 1.07$). Detection of such short molecules has previously been possible in voltage-driven translocation experiments only in the case of molecule slowing by strong and highly fluctuating interactions with the pore walls[18] that yield extremely broad time distributions, preventing accurate length discrimination or resolution.

Another advantage of using a pressure bias to capture molecules is the ability to study neutral molecules. We explored the detection and characterization of nominally neutral polyethylene glycol (PEG) with a nanopore, and we were surprised to discover that the molecule appears to carry a small positive charge. The evidence for this was that for $\Delta P = 1.03$ atm and $V = -100$ mV, we observed no events distinguishable from noise, but when the voltage bias was reversed to +100 mV translocation events were easily observed and resolved (Figure 4 inset). This can be understood if the translocation times were shorter than the time resolution of our electronics for the negative bias, so the molecule's speed could not be resolved. However, for the positive bias, pressure-derived and voltage-derived forces were now nearly balanced and the molecule was slowed enough so its signal could be resolved. We conclude that PEG must carry a small positive charge. Figure 4 shows a scatter plot of 77 translocation events of 12 kDa PEG molecules at pH 4.2, an applied pressure of $\Delta P = 1.03$ atm and $V = +100$ mV. The rms noise level was 8.0 pA with a 20 kHz hardware filter. The broad translocation distribution seen in Figure 4 may be due to strong interactions with the pore surface, not surprising considering the use of PEG as a glass surface treatment.

These results allow an estimate of the charge of the 12 kDa PEG molecule in the pore by an approach similar to that used in the Millikan oil drop experiment,[19] in which the pressure-derived and voltage-derived forces are balanced to maximize the translocation time. The charge can be deduced from the balance of forces on the molecule via $qE = F_{mech}$, where E is the electric field in the pore and F_{mech} is the sum of the mechanical forces on the molecule from the applied pressure and/or the fluid flow through the pore. The hydrodynamic forces on a polymer confined in a nanopore are complex to calculate, but the upper and lower bounds of the PEG charge are

easily estimated. These bounds correspond to the limits in which an immobilized PEG molecule maximally or minimally blocks the fluid flow through the nanopore.

From the ionic conductance of the pore we deduce its radius to be 4.0 nm, assuming that the pore has a conical shape such that it is equivalent to a cylindrical pore of length 30 nm.[20] This radius is about the same as the radius of gyration of 12 kDa PEG (3.2 nm, based on a monomer length of 0.35 nm and a persistence length of 0.38 nm[21]), so the polymer should occupy a significant fraction of the cross-section of the pore. Assuming that the polymer completely blocks fluid flow through the nanopore, the entire pressure drop, $\Delta P = 1.03$ atm, is across the polymer. The mechanical force is $F_{mech} = \pi R^2 \Delta P$, where R is the pore radius. The upper bound to the PEG charge is $q_{max} = \pi \Delta P R^2 L / V = 9.8e$, where we have substituted $E = V / L$ for the electric field, $V = 100$ mV is the applied voltage, and $L = 30$ nm is again the pore length.

Alternatively, if the molecule did not block the fluid flow at all, the mechanical force would be the Stokes drag $F_{mech} = \gamma \overline{v}$, where $\gamma = 6\pi \eta R_H$ is the Stokes drag coefficient of a sphere of hydrodynamic radius R_H in a fluid of viscosity η and average fluid velocity $\overline{v}$. To estimate R_H, we note that the diffusion constant $D \approx 7.7 \times 10^{-11}$ m^2/s is available for a free 12 kDa PEG molecule in heavy water at 33 °C.[22] Applying the Stokes-Einstein relation $D = k_B T / 6\pi \eta R_H$, we find that $R_H \approx 3.2$ nm. The average fluid velocity under Poiseuille flow is $\overline{v} = \Delta P R^2 / 8\eta L$. The charge is then $q_{min} = \gamma \overline{v} / E = 3\pi R^2 R_H \Delta P / (4V) = 0.8e$. Note that $q_{min} = q_{max} (3R_H / 4L)$. This estimate of the charge is a lower bound because it does not account for the enhanced drag from confinement of the polymer in the nanopore.

So far we have not considered the potential influence of electroosmotic flow (EOF) on the estimates of the PEG charge. EOF arises from the action of the electric field on mobile

counterions that have accumulated near the charged surface of the pore. Previous work on the surface charge of silicon nitride nanopores[23] shows that the point of zero charge of the silicon nitride surface is pH ≈4.6. At pH 4.2 the surface carries only a very small positive charge ($\approx 10^{12}$ e/cm^2). The techniques in Ref. [23] predict that the electroosmotic velocity in this experiment is about 15% of the average Poiseuille flow velocity ($\bar{v} \approx 7$ mm/s) and in the same direction. This justifies neglecting EOF in our estimates of the PEG charge. Because the EOF is in the same direction as the pressure-driven flow, it does not contribute to the slowing of the PEG molecule by the electric field.

We note that a positive charge on PEG has also been reported from studies using protein nanopores.[24, 25] The very different physics and experimental conditions involved make it difficult to relate these measurements to those reported here.

Finally, we wish to comment on the utility of pressure-driven translocation for speed control in various applications. A number of speed control mechanisms for DNA have been implemented in solid state nanopores.[16, 18, 26, 27] The pressure method combines many of the best qualities of these, in that the equipment is inexpensive, the translocation time distributions are narrow, the dynamic range is larger than an order of magnitude, and the capture rate is unaffected. Like all strategies for slowing by reducing the net force on the DNA molecule, however, this technique is subject to the thermal fluctuations described previously.[17] We therefore expect that force-balanced translocation will find more application in the detection of small molecules, including discrimination among populations of proteins or short DNA strands.

The data and discussion presented above demonstrate that modest pressures applied to a voltage-biased nanopore greatly extend their utility as single molecule detectors by enabling neutral molecule capture and detection, as well as control of molecule translocation speeds

through the pore. We demonstrate nearly an order-of-magnitude improvement in length discrimination, which can be further improved in combination with other methods. This broader range of detectable molecule sizes, charge states, and spatial conformations considerably expands the applicability of nanopore detection technologies. In particular, we anticipate these advances to be important for single-molecule studies of a wide array of proteins. Refined experiments should also allow the accurate determination of the macromolecule charges in the nanopore. Perhaps the greatest current challenge to the routine practical application of the methods demonstrated in our work is the lack of control and understanding when direct chemical interactions between translocating molecules and the wall of the nanopore are important. While these interactions still allow detection of molecules using these methods, they limit the effective lifetime of the nanopore and thereby the amount of data that can be collected. Nanopores in well characterized, or functionalized, membranes may enable these forces to be used to greater advantage in the art of nanopore science.

Methods. *Nanopore fabrication.* Thin films of 2 µm wet thermal silicon oxide and 100 nm LPCVD low-stress (silicon-rich) silicon nitride were deposited on 500-µm thick P-doped <100> Si wafers of 1-20 ohm-cm resistivity. Freestanding 20-µm membranes were formed by anisotropic KOH (33%, 80 °C) etching of wafers in which the thin films had been removed in a photolithographically patterned region by reactive ion etch. A focused ion beam (Micrion 9500) was used to remove about 1.5 µm of silicon oxide in a 1 µm square area in the center of the freestanding membrane; a subsequent timed buffered oxide etch (BOE) removed about 600 nm of the remaining oxide, leaving a 2-µm free-standing "minimembrane" of silicon nitride in the center of the freestanding oxide/nitride membrane. The nitride film is about 80 nm thick after processing in KOH and BOE, as measured by ellipsometry and cross-sectional transmission

electron microscopy (TEM). A focused 200-keV electron beam from a JEOL 2010F field-emission TEM (JEOL USA, Peabody, MA) was used to form[12] roughly hourglass-shaped[20] nanopores in the center of the nitride minimembrane. Nanopore diameters were approximately 10 nm.

DNA preparation. The 3270 bp (3.27 kbp) circular plasmid vector pENTR／D－TOPO was prepared from *E. coli* using a CWBIO[®] PurePlasmid Mini Kit (Beijing CoWin Bioscience Co., Ltd., Beijing, China) and linearized by digestion with EcoRV restriction endonuclease. DNA fragments of 615 bp and 1140 bp (1.14 kbp) were produced from an *Arabidopsis thaliana* cDNA library by polymerase chain reaction. All lengths were purified using Invitrogen® Purelink[TM] Quick Gel Extraction and PCR Purification Combo Kit (Life Technologies Corp., Grand Island, NY) following gel electrophoresis.

DNA translocation measurements. Each sample was mounted in a sealed cell such that the freestanding membrane containing the nanopore separates two electrically isolated reservoirs of 1.6 M KCl maintained at pH 9 by 10 mM Tris and 1 mM EDTA buffer, unless otherwise specified. The cell was capable of withstanding several atmospheres of internal pressure. Using estimates of the Young's modulus and yield strength of silicon nitride as 300 GPa and 0.6 GPa,[28] respectively, we estimate that the thin membranes are capable of withstanding over 40 atm of pressure without mechanical failure.[29] As discussed above, however, the pressures required to offset a given voltage is proportional to the square of the pore radius. Because an exceptionally robust flow cell is required to apply the high pressures required for small pores, we use relatively large (10 nm) pores and modest pressures for this preliminary work. Pressure was applied to either side of the nanopore using a regulated tank of compressed nitrogen or regulated compressed air; the pressure was read using a pressure meter with a nominal precision of 0.5%

(about 0.01 atm). The opposite side of the membrane was maintained at atmospheric pressure (see Figure 1a). DNA was diluted to about 2 ng/µL in the buffer solution and introduced into the sample cell, which was then sealed so pressure could be applied. All electrical measurements were carried out inside a dark Faraday cage with external circuitry coupled to the electrolyte reservoirs with Ag/AgCl electrodes. An Axopatch 200B patch-clamp amplifier (Molecular Devices, Sunnyvale, CA), operating in resistive feedback mode with an 8-pole, 40-kHz, low pass Bessel filter, was used for measuring ionic currents and applying voltage biases. All rms noise levels refer to an integration of the current noise power spectrum between 200 Hz and 40 kHz. All voltages are referenced to the high-pressure side of the nanopore, where the molecules are injected; for negatively charged molecules such as DNA, negative voltages retard translocation, while positive voltages facilitate translocation. The amplifier output was digitized at 250 kHz to reduce aliasing and continuously recorded to disk using a Digidata 1440A digitizer and pClamp 10 software. The digitized ionic current signals were processed using custom MATLAB code (The MathWorks, Natick, MA) that fits each event to a series of sharp current steps modified by the transfer function of the experimental low-pass filter.
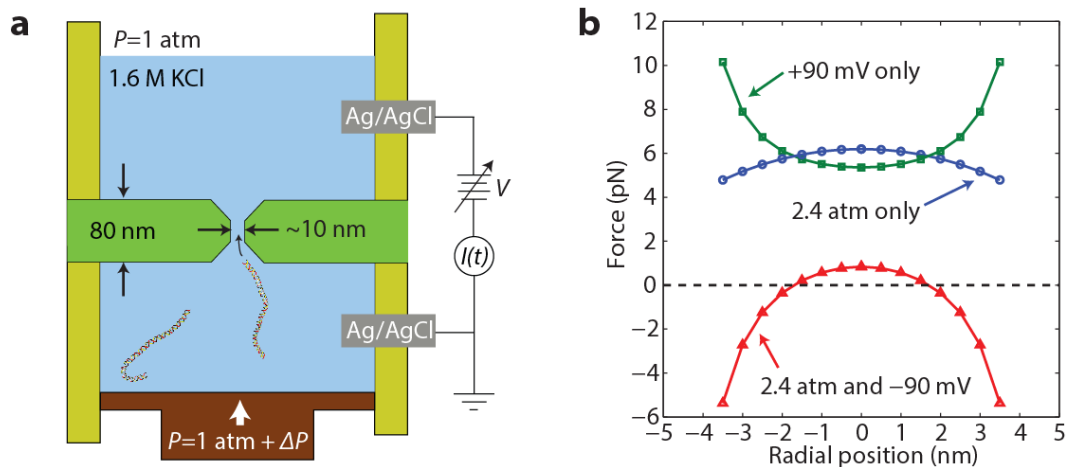
Figure 1. (a) Schematic of DNA translocation experiment with variable voltage and pressure. (b) Calculated driving force profile on dsDNA as a function of off-center position inside a cylindrical nanopore of radius 5 nm in 1.6 M KCl at pH 9 under pressure-derived forces, electrical forces, and an opposing combination of the two. Positive forces drive the DNA through the nanopore.
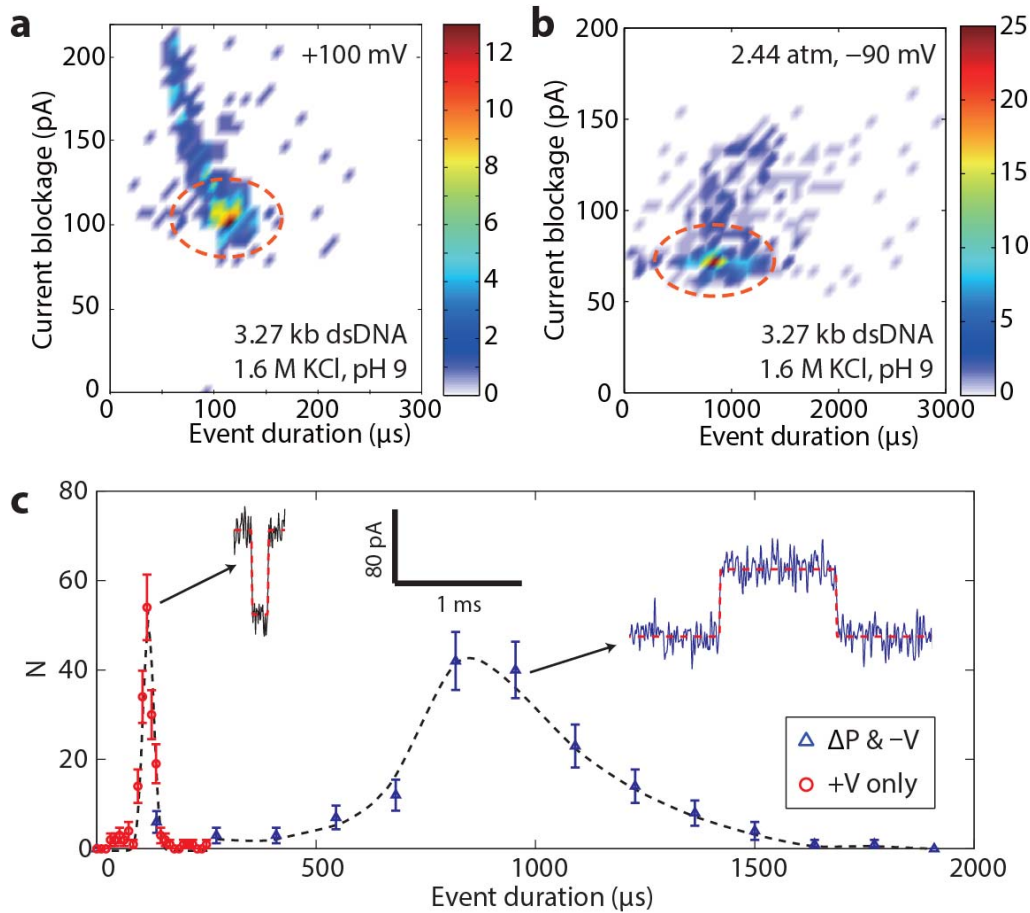
Figure 2. (a) Density histogram of 3.27 kb dsDNA translocations driven by $V = +100$ mV. (b) Density histogram of 3.27 kb dsDNA translocations driven by $\Delta P = 2.44$ atm and $V = -90$ mV in a similarly sized nanopore. The red circles indicate the unfolded molecule translocation events. (c) Unfolded event duration histograms from (a) and (b). The dashed lines are guides to the eye. Insets: typical events from voltage-driven and pressure-driven experiments. The dashed lines represent the fits from which the event durations are determined.
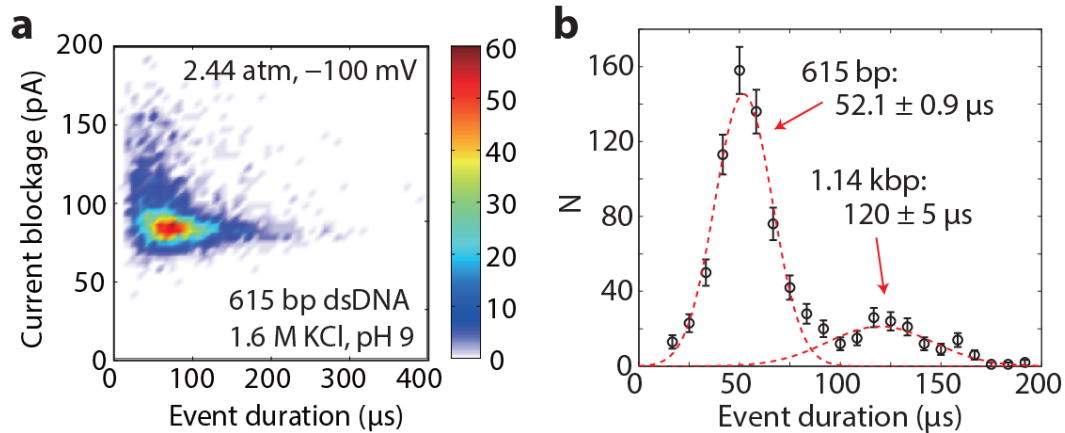
Figure 3. Detection and discrimination of short dsDNA molecule lengths. (a) Density histogram of 615 bp dsDNA translocations driven by $\Delta P = 2.44$ atm and $V = -100$ mV. (b) Demonstration of length discrimination between 615 bp and 1.14 kbp dsDNA molecules at $\Delta P = 2.56$ atm and $V = -100$ mV. The means of the weighted Gaussian fits (dashed lines) are shown in the figure; the standard deviations are 14.2 ± 0.8 µs and 26 ± 4 µs, respectively.
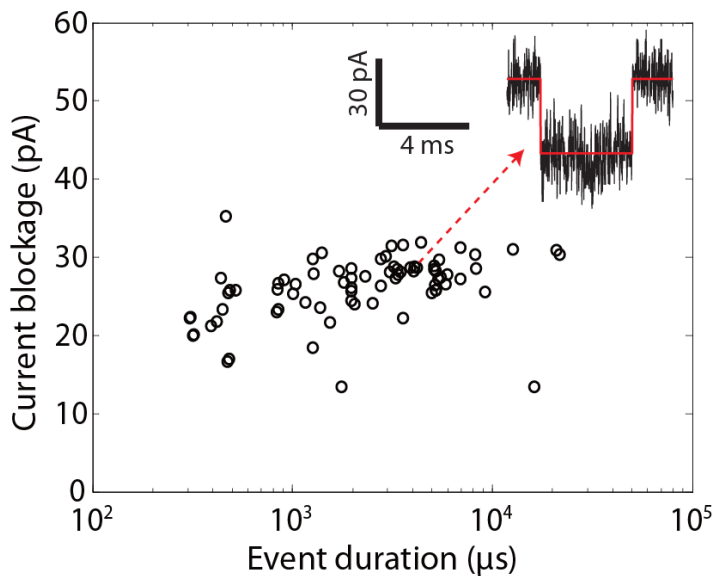

Figure 4. Scatter plot of 12 kDa PEG events (77 total) at $V = +100$ mV driven by $\Delta P = 1.03$ atm in 1.6 M KCl at pH 4.2. Inset: typical event for pressure-driven translocation of PEG. Events at $V = -100$ mV were detected as filter-limited spikes and are not shown.

15

ASSOCIATED CONTENT

Supporting Information

Current trace data supporting Figures 2a-b, as well as a discussion of noise considerations in these experiments, are included in the Supporting Information, which is available free of charge via the Internet at http://pubs.acs.org.

AUTHOR INFORMATION

Corresponding Author

*Corresponding authors: zhaoqing@pku.edu.cn; yudp@pku.edu.cn; golovchenko@physics.harvard.edu.

Author Contributions

‡These authors contributed equally to this work.

Notes

The authors declare no competing financial interests.

under the direction of Q. Z. and D. Y.; D. P. H., and J. G provided guidance and suggestions. Z. T. prepared the DNA. B. L. analyzed the data. B. L., D. P. H., and Q. Z. performed finite element simulations. B. L., D. P. H., and J. G. co-wrote the final paper. All authors commented on the manuscript. B. L. and D.P.H. contributed equally to this work.

REFERENCES

(1)   Li, J.; Stein, D.; McMullan, C.; Branton, D.; Aziz, M. J.; Golovchenko, J. A. *Nature* **2001,** 412, 166-169.

(2)   Talaga, D. S.; Li, J. *J. Am. Chem. Soc.* **2009,** 131, 9287-9297.

(3)   Dekker, C. *Nat. Nanotechnol.* **2007,** 2, 209-215.

(4)   Branton, D.; Deamer, D. W.; Marziali, A.; Bayley, H.; Benner, S. A.; Butler, T.; Di Ventra, M.; Garaj, S.; Hibbs, A.; Huang, X. H.; Jovanovich, S. B.; Krstic, P. S.; Lindsay, S.; Ling, X. S. S.; Mastrangelo, C. H.; Meller, A.; Oliver, J. S.; Pershin, Y. V.; Ramsey, J. M.; Riehn, R.; Soni, G. V.; Tabard-Cossa, V.; Wanunu, M.; Wiggin, M.; Schloss, J. A. *Nat.Biotechnol.* **2008,** 26, 1146-1153.

(5)   Li, J.; Gershow, M.; Stein, D.; Brandin, E.; Golovchenko, J. A. *Nat. Mater.* **2003,** 2, 611-615.

(6)   van den Hout, M.; Vilfan, I. D.; Hage, S.; Dekker, N. H. *Nano Lett.* **2010,** 10, 701-707.

(7)   Storm, A. J.; Storm, C.; Chen, J.; Zandbergen, H.; Joanny, J. F.; Dekker, C. *Nano Lett.* **2005,** 5, 1193-1197.

(8)   Olasagasti, F.; Lieberman, K. R.; Benner, S.; Cherf, G. M.; Dahl, J. M.; Deamer, D. W.; Akeson, M. *Nat. Nanotechnol.* **2010,** 5, 798-806.

(9)   Derrington, I. M.; Butler, T. Z.; Collins, M. D.; Manrao, E.; Pavlenok, M.; Niederweis, M.; Gundlach, J. H. *P. Natl. Acad. Sci. USA* **2010,** 107 16060-16065.

(10)   Cherf, G. M.; Lieberman, K. R.; Rashid, H.; Lam, C. E.; Karplus, K.; Akeson, M. *Nat. Biotechnol.* **2012,** 30, 344-348.

(11)   Manrao, E. A.; Derrington, I. M.; Laszlo, A. H.; Langford, K. W.; Hopper, M. K.; Gillgren, N.; Pavlenok, M.; Niederweis, M.; Gundlach, J. H. *Nat. Biotechnol.* **2012,** 30, 349-353.

(12)   Storm, A. J.; Chen, J. H.; Ling, X. S.; Zandbergen, H. W.; Dekker, C. *Nat. Mater.* **2003,** 2, 537-540.

(13)   Lu, B.; Hoogerheide, D. P.; Zhao, Q.; Yu, D. P. *Phys. Rev. E* **2012,** 86, 011921.

(14)   Ghosal, S. *Phys.Rev. Lett.* **2007,** 98, 238104.

(15)   van Dorp, S.; Keyser, U. F.; Dekker, N. H.; Dekker, C.; Lemay, S. G. *Nat. Phys.* **2009,** 5, 347-351.

(16)   Fologea, D.; Uplinger, J.; Thomas, B.; McNabb, D. S.; Li, J. *Nano Lett.* **2005,** 5, 1734-1737.

(17)   Lu, B.; Albertorio, F.; Hoogerheide, D. P.; Golovchenko, J. A. *Biophy. J.* **2011,** 101, 70-79.

(18)   Wanunu, M.; Sutin, J.; McNally, B.; Chow, A.; Meller, A. *Biophys. J.* **2008,** 95, 4716-4725.

(19)   Millikan, R. A. *Phys. Rev.* **1913,** 2, 109-143.

(20)   Kim, M. J.; McNally, B.; Murata, K.; Meller, A. *Nanotechnology* **2007,** 18, 205302.

(21)   Kienberger, F.; Pastushenko, V. P.; Kada, G.; Gruber, H. J.; Riener, C.; Schindler, H.; Hinterdorfer, P. *Single Mol.* **2000,** 1, 123-128.

(22)   Tanner, J. E.; Liu, K. J.; Anderson, J. E. *Macromolecules* **1971,** 4, 586-588.

(23)   Hoogerheide, D. P.; Garaj, S.; Golovchenko, J. A. *Phys. Rev. Lett.* **2009,** 102, 256804.

(24)   Rodrigues, C. G.; Machado, D. C.; Chevtchenko, S. F.; Krasilnikov, O. V. *Biophys. J.* **2008,** 95, 5186-5192.

(25)   Reiner, J. E.; Kasianowicz, J. J.; Nablo, B. J.; Robertson, J. W. F. *P. Natl. Acad. Sci. USA* **2010,** 107, 12080-12085.

(26)   Kowalczyk, S. W.; Wells, D. B.; Aksimentiev, A.; Dekker, C. *Nano Lett.* **2012,** 12, 1038-1044.

(27)   Keyser, U. F.; Koeleman, B. N.; Van Dorp, S.; Krapf, D.; Smeets, R. M. M.; Lemay, S. G.; Dekker, N. H.; Dekker, C. *Nat.Phys.* **2006,** 2, 473-477.

(28)   Shackelford, J. F.; Alexander, W., *CRC Materials Science and Engineering Handbook.* 3rd ed.; CRC Press: Boca Raton, FL, 2001.

(29)   Schomburg, W. K., *Introduction to Microsystem Design.* Springer: New York, 2011.

Pressure-controlled motion of single polymers in solid-state nanopores

Bo Lu[1]‡, David P. Hoogerheide[2]‡, Qing Zhao[1],*, Hengbin Zhang[1], Zhipeng Tang[1], Dapeng Yu[1],*, and Jene A. Golovchenko[2],*

[1]State Key Laboratory for Mesoscopic Physics and Electron Microscopy Laboratory, School of Physics, Peking University, Beijing 100871, People's Republic of China

[2]Department of Physics, Harvard University, Cambridge, Massachusetts 02138, USA

‡These authors contributed equally to this work.

*Corresponding authors: zhaoqing@pku.edu.cn; yudp@pku.edu.cn; golovchenko@physics.harvard.edu

S1. Representative data

Here we present current traces and typical events for the data in Figure 2a and 2b.
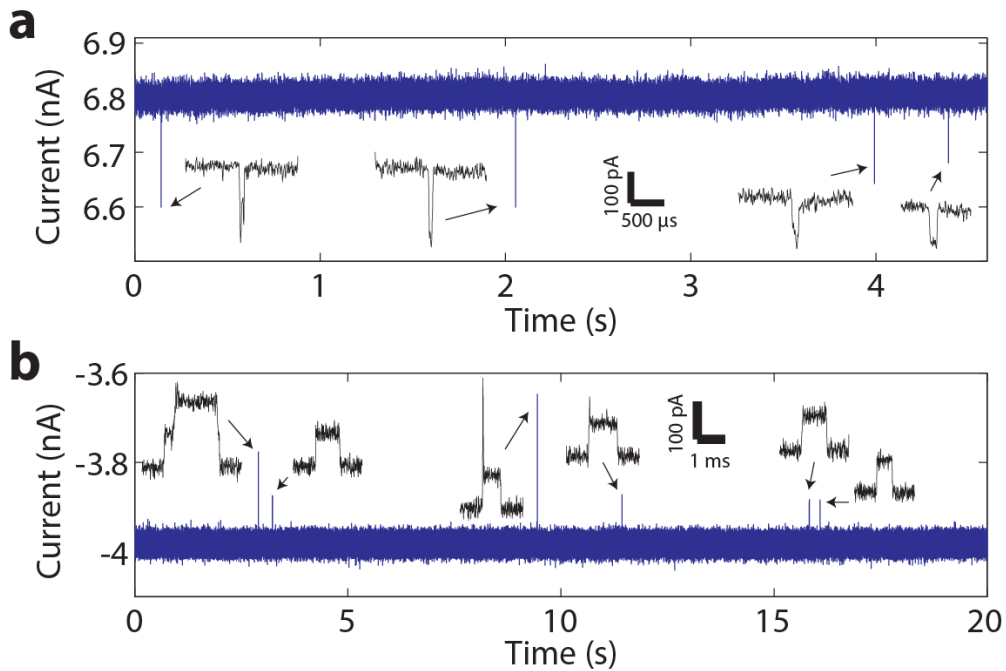
Figure S1. (a) A section of the current trace used to generate the density histogram in Figure 2a, with typical events. (b) A section of the current trace used to generate the density histogram in Figure 2b, with typical events.

S2. Noise considerations

Here we present a noise power spectrum for the data presented in Figure 2b. All data were hardware filtered with an 8-pole low-pass Bessel filter at 40 kHz (except for the PEG experiments in Figure 4, which were filtered at 20 kHz) and digitized at 250 kHz. Because different experiments were done at different gain levels, all data presented in the paper are software filtered with an 8-pole low-pass Bessel filter at 80 kHz (well above the amplifier bandwidth), to remove unwanted high-frequency components. This allows more meaningful comparison of the noise levels shown in current traces and sample events. In addition, to standardize the comparison of noise levels in different pores, all rms noise levels are calculated by integrating the current noise power spectrum between 200 Hz and 40 kHz, as shown in Figure S2.

These experiments were optimized for time resolution. Similar voltages are used in typical voltage-biased translocation experiments as in the pressure-biased experiments, so the current blockage and noise levels are comparable to those of typical translocation experiments. In principle, the long translocation times of pressure-biased experiments allow the use of more aggressive filtering, significantly improving the ratio between the current blockage and the rms noise.
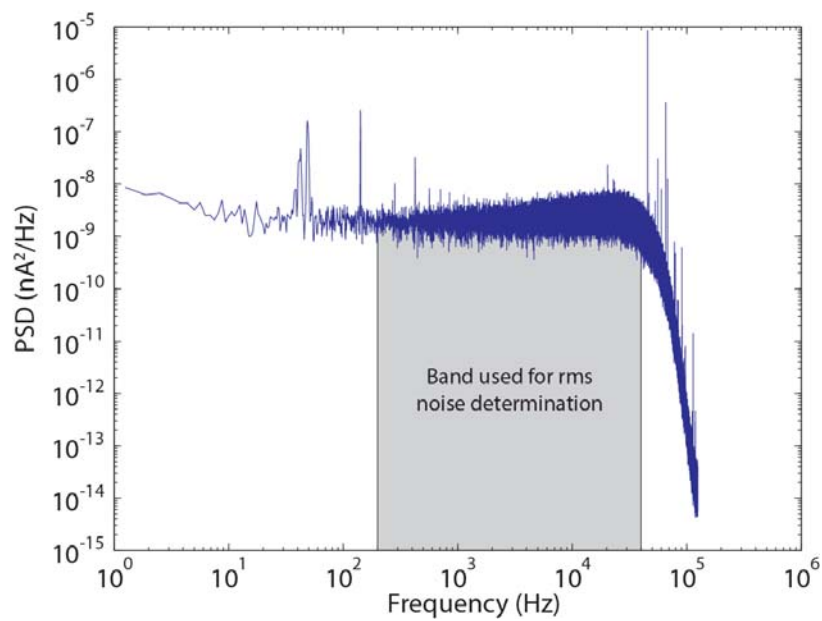
Figure S2. Power spectrum for the data in Figure 2b, showing the band used to calculate the rms noise level.